

## Molecular simulation strategy for mechanical modeling of amorphous/porous low-dielectric constant materials

Cadmus A. Yuan,<sup>1,a)</sup> Olaf van der Sluis,<sup>1,b)</sup> G. Q. Zhang,<sup>1,c)</sup> Leo J. Ernst,<sup>1</sup> Willem D. van Driel,<sup>2</sup> Amy E. Flower,<sup>3,d)</sup> and Richard B. R. van Silfhout<sup>3</sup>

<sup>1</sup>Department of Precision and Microsystem Engineering, Delft University of Technology, 2628 CD Delft, The Netherlands

<sup>2</sup>NXP Semiconductors, Gerstweg 2, 6534 AE, Nijmegen, The Netherlands

<sup>3</sup>Philips Applied Technologies, High Tech Campus 7, 5656 AE, Eindhoven, The Netherlands

(Received 13 June 2007; accepted 5 December 2007; published online 14 February 2008)

We propose an amorphous/porous molecular connection network generation algorithm for simulating the material stiffness of a low- $k$  material (SiOC:H). Based on a given concentration of the basic building blocks, this algorithm will generate an approximate and large amorphous network. The molecular topology is obtained by distributing these blocks randomly into a predefined framework. Subsequently, a structural relaxation step including local and global perturbations is applied to achieve the most likely stereochemical structure. Thus, the obtained mechanical properties of the low- $k$  materials have been verified with the experimental data. © 2008 American Institute of Physics. [DOI: 10.1063/1.2832639]

Because advanced integrated circuit (IC) technologies demand the minimization of the intrinsic delay of signal propagation, industries are replacing aluminum with copper traces and developing alternative materials with a lower dielectric constant ( $k$  value) than that of the currently used one.<sup>1,2</sup> Silicon oxide based low- $k$  materials are preferred because the fabrication processes for these materials exhibit high IC compatibility with a high yielding rate. Black diamond (BD), a carbon doped silicon oxide deposited at 350 °C by plasma enhanced chemical vapor deposition<sup>2</sup> and chemically denoted as SiOC:H, is one of the silicon based low- $k$  materials and belongs to the organosilicate glasses (OSG). It contains a silica backbone and characteristic Si-CH<sub>3</sub> terminating groups, with the general stoichiometric ratio (CH)<sub>3</sub>SiO<sub>3/2</sub>, as illustrated in Fig. 1. The different groups (building blocks) are defined as the number of O atoms linked to a Si atom: zero (Z), mono (M), di (D), tri (T), and quad (Q). The bond terminators are of the type Si-R, where R is the -CH<sub>3</sub>, -O, and -OH functional group. For simplicity, direct Si-Si bonds and the terminators -H, -OH, and -O are not considered.<sup>3</sup> Based on the experimental results,<sup>4</sup> the pore size is assumed to be building block.

Delamination at the interfaces with low- $k$  material is a critical issue for the reliability of IC backend structures.<sup>4,5</sup> Experiments<sup>5,6</sup> exhibit a trend of improving the mechanical properties by modifying the chemical composition. However, the relationship between the chemical composition to the mechanical properties of the SiOC:H from different fabrication processes/precursors/treatments is still unclear. A precise molecular model capable of describing the amorphous and porous nature of OSG on a large scale is required.

Herein, we propose an amorphous/porous OSG generating algorithm, using the experimentally obtained concentrations of the basic building blocks and the porosity. The real fabrication process of the material is not modeled due to the complexity. However, the technique of the hand-built random network model<sup>7-9</sup> is not used because the system consists of several basic building blocks.

The local/global algorithm including the connection network (for molecular topology) and the potential energy minimization (for stereochemistry) steps will be described, concluding with the experimental validation.

A predefined framework, which is made up of SiO<sub>2</sub> tetrahedral sharing corners, is established [Fig. 2(a)]. The nodes (gray spheres) and links (red lines) are possible locations of the basic building blocks and the possible links (Si-O-Si bonds) between these blocks, respectively. Within this framework, each node has four links connected to it. The geometrical distance between two nodes is approximately defined as 0.3 nm. The distribution of the building blocks obeys the following rules:

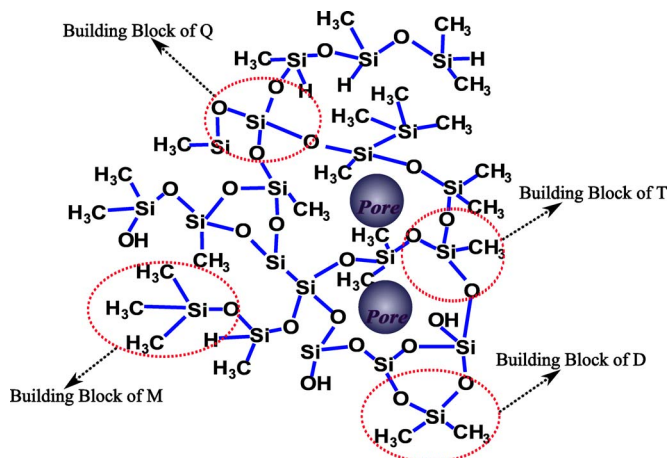


FIG. 1. (Color online) Chemical structure of SiOC:H. The basic building blocks of Q (left-upper panel), T, D, and M are illustrated around the periphery of the molecule illustration in a clockwise direction. The pores are also shown.

<sup>a)</sup> Author to whom correspondence should be addressed. Present address: Mekelweg 2, 2628 CD Delft, The Netherlands. Electronic mail: c.a.yuan@tudelft.nl.

<sup>b)</sup> Also at Philips Applied Technologies, The Netherlands.

<sup>c)</sup> Also at NXP Semiconductors, The Netherlands.

<sup>d)</sup> Also at Department of Mechanical Engineering, Georgia Institute of Technology, Atlanta, GA, USA.

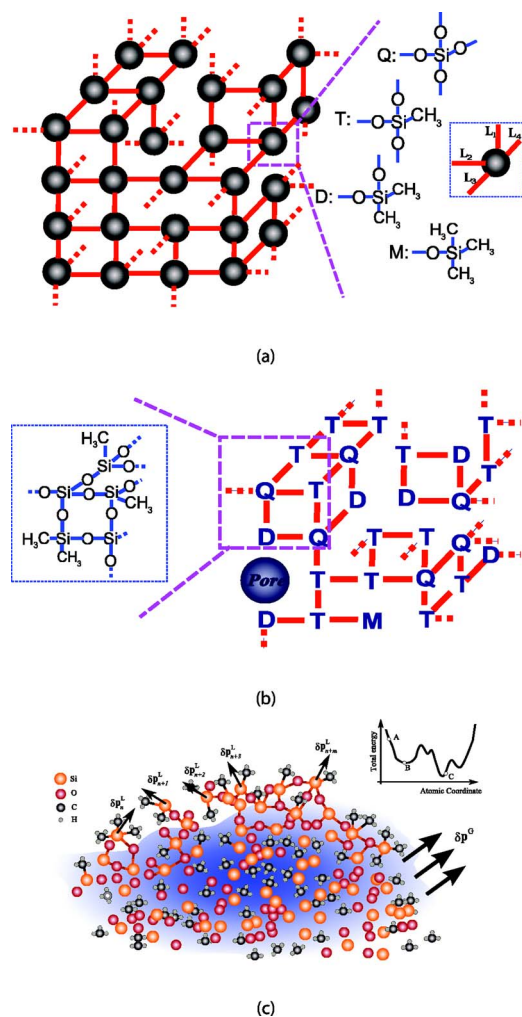


FIG. 2. (Color online) Generating algorithm of SiOC:H. (a) is the pre-defined framework. The nodes will be replaced by either Q, T, D, M, or pore. (b) shows the obtained molecular topology and right panel of (b) shows the atomic chemical connection. (c) shows the concept of global/local molecular optimization in the molecule and in scheme (inset), where A, B, and C denote the initial state, local minimal, and global minimal, respectively.

- Chemical nature of building blocks: When a pore, Q, T, D, or M is distributed onto the node, the total number of links for that node is fixed to zero, four, three, two, or one, respectively. In other words, for each node, the spare links [e.g.,  $L_4$  in the inset of Fig. 2(a)] are randomly terminated from the former linkage status ( $L_{1,2,3,4}$ ).
- Average distribution: A local high concentration of a specific type of building block should be prevented.
- Minimal numbers of dangling bonds: Because the dangling bonds are not physically favored, reducing them will easily lead to a minimum potential energy state.

A random number generator is introduced to decide which links will be terminated and to obtain an average distribution. Manipulations are applied to reduce the number of dangling bond, such as establishing a chemical bond between two dangling bond when these two bonds are close to each other (within 1.5–2 nm). Hydrogen is appended to the dangling bond which cannot be reduced.

Subsequently, the energy minimization procedure is applied onto the obtained topology [Fig. 2(b)] resulting in the

most likely stereochemical structure. The minimization step comprises continuous iterations of the local perturbation of the atom coordinate and the global perturbation of the system [Fig. 2(c)]. Local optimization consists of (i) the local perturbation of the atom coordinates ( $\delta P_n^L \cdots \delta P_{n+m}^L$ ), (ii) energy evaluation of the given conformation, and (iii) conformation adjustment of atomic coordinates. Local minimization can lead the system to approach a local minimum, which may not correspond to the global minimum,<sup>10</sup> as illustrated in the inset of Fig. 2(c). Hence, global perturbation of the system ( $\delta P^G$ ) is needed especially for achieving the stress-free state of a large OSG molecule. This can be achieved simply by applying a small displacement or a quench loading onto the system for mechanical and thermal simulation. The molecular structural minimization is converged if the reaction force is (nearly) zero, while mechanically clamping the model at two opposite ends.

In order to predict Young's modulus of the molecule, a bar shaped molecular model is established.<sup>11</sup> Along the longitudinal direction, one end of the model is fixed in all degrees of freedom and a displacement with a constant velocity is applied to the opposite end (which is illustrated in the inset).<sup>11</sup> The Young's modulus can be deduced by  $E = L_0^2 / V_0 (\Delta F / \Delta d)$ ,<sup>12</sup> where  $F$ ,  $\Delta d$ ,  $L$ , and  $V$  are the reaction force, applied displacement, initial length, and initial volume of the specimen, respectively. For our calculations, the commercial solver Discover<sup>13</sup> is used with the COMPASS force field (definition:cff91, Version 2.6) (Ref. 14) at 300 K.

A molecular model with 1224 building blocks is used. A T-rich SiOC:H molecule before UV treatment, with concentrations of Q, T, D, and pore as 16.3%, 46.3%, 31.3%, and 6.0% (porosity) measured by NMR,<sup>6</sup> is modeled. Note that the molecular model illustrated in Fig. 3(a) is the one before the local/global optimization procedure. Another molecular model based on the SiOC:H after UV treatment, with respective concentrations of 23.2%, 48.2%, 21.2%, and 7.4% (porosity), is established. Figure 3(c) shows that if the local/global optimization is not performed, the model which is clamped at two opposited ends, exhibits a reaction force of 75 nN without any applied external displacement. Next, the model is loaded, which is illustrated in the inset of Fig. 3(d). The simulated Young's moduli for molecular models before and after UV treatment is 14.3 and 19.0 GPa, which resemble the experimental results of 11.0 and 16.0 GPa, where the porosities are 7.0% and 8.0%.<sup>6</sup> The average pore size in the model is approximately 0.8 nm in diameter, while the experiment shows 1.5–2.0 nm.<sup>15</sup>

When the model size is large enough, the effect of the local randomization of the basic building blocks is averaged out. Sensitivity analysis of the random generator shows that the fluctuation of Young's modulus is approximately no more than 7.0% for the molecular model before and after UV treatment. Moreover, we conducted a series of simulations and obtained the sensitivity of the Young's modulus ( $E$ ) with respect to the different building block concentrations. These simulation results can be expressed by a fitting equation:  $E(r_Q, r_T, r_D) = E_Q r_Q + E_T r_T + E_D r_D$ , where  $E_{Q,T,D}$  are the fitting coefficients and  $r_{Q,T,D}$  are the concentration of basic building blocks of Q, T, and D. The approach is based on the rule of mixtures. Here, isotropic behavior, valid for random structures, and no interaction between the individual constituents, is assumed for the fitting equation.<sup>16</sup> The pore concentration is not considered in the previous equation because the pore

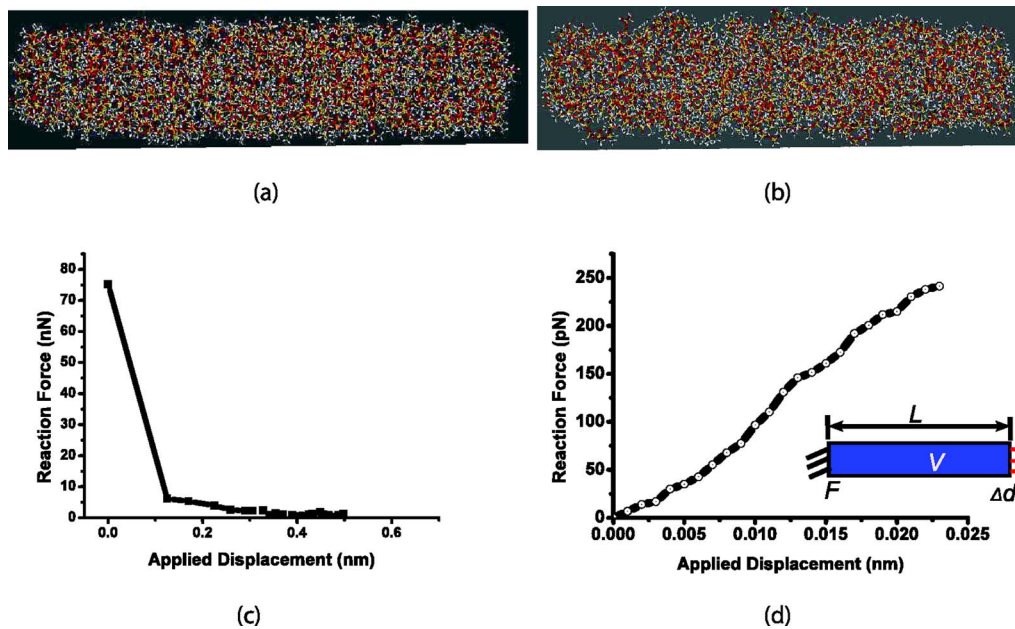


FIG. 3. (Color online) Simulation result of SiOC:H before UV treatment. (a) is the molecular model without local/global optimization. (b) is the molecular model with most likely stereochemistry. (c) is the curve of reaction force and applied displacement during the structural minimization. (d) shows the reaction force curve of the model where the boundary condition is illustrated in the inset.

does not contribute to the mechanical stiffness. However, the equation of  $r_Q + r_T + r_D + r_{\text{pore}} = 1$  where  $r_{\text{pore}}$  is the porosity, holds. The coefficients are listed in Table I. The  $E_Q$  and  $E_T$  can be physically interpreted as Young's modulus of the amorphous silica and T-rich methylsilsesquioxane (MSQ). To validate our results, experimentally determined stiffness values of these individual materials are compared with our numerically determined values, and can be found in Table I. The simulation results  $E_Q$  and  $E_T$  approach Young's moduli of amorphous silica (TEOS) before annealing<sup>17</sup> and MSQ without porosity.<sup>18</sup> As listed in Table I, the simulated  $E_Q$  and  $E_T$  are close to the experimental results. Note that the fitting coefficient of  $E_D$  is 2.0 GPa. It can be concluded that our numerical values are rather accurate and thus confirm the proposed approach, even though TEOS, BD, and MSQ have different processes, precursor and treatments. Moreover, the OSG material shows molecular similarity, due to the similar predefined framework used in the modeling.

An algorithm, which can generate a molecular structure of amorphous/porous organosilicate glasses, is presented for the prediction of the material's mechanical properties. It is comprised of two steps: generating a molecular topology and obtaining the most likely stereochemical structure. A parametric study is performed by which the mechanical behavior of the low- $k$  material is established. Comparison with experimental stiffness values confirm the accuracy of our method.

TABLE I. Fitting coefficients

	Coefficients	
	$E_Q$	$E_T$
Young's modulus (GPa)	56.9	16.7
Physical interpretation	Amorphous silica	MSQ without porosity
Measurement results (GPa)	56.0 <sup>a</sup>	15.2 <sup>b,c</sup>

<sup>a</sup>Reference 16.

<sup>b</sup>Reference 17.

<sup>c</sup>Reference 18.

This chemical-mechanical relationship of low- $k$  material will provide a clear picture for designing a more reliable material for the practical IC backend structure.

The authors thank Professor B. J. Thijsse (TU Delft, Netherlands) for valuable discussion on the amorphous algorithm. C.A.Y. thanks Dr. C. Menke and Dr. J. Wescott (Accelrys, UK) for discussions on numerical simulation techniques.

- <sup>1</sup>International Technology Roadmap for Semiconductors, ITRS, 2006.
- <sup>2</sup>N. Chèrault, G. Carlotti, N. Casanova, P. Gergaud, C. Goldberg, O. Thomas, and M. Verdier, *Microelectron. Eng.* **82**, 368 (2005).
- <sup>3</sup>S. K. Estreicher, *Phys. Rev. B* **41**, 9886 (1990).
- <sup>4</sup>A. Humbert, D. E. Badaroglu and R. J. O. M. Hoofman, *Mater. Res. Soc. Symp. Proc.* **914**, 0914-F04-03 (2006).
- <sup>5</sup>R. J. O. M. Hoofman, G. J. A. M. Verheijden, J. Michelon, F. Iacopi, Y. Travalay, M. R. Baklanov, Zs. Tökei, and G. P. Beyer, *Microelectron. Eng.* **80**, 337 (2005).
- <sup>6</sup>F. Iacopi, Y. Travalay, B. Eyckens, C. Waldfried, T. Abell, E. P. Guyer, D. M. Gage, R. H. Dauskardt, T. Sajavaara, K. Houthoofd, P. Grobet, P. Jacobs, and K. Maex, *J. Appl. Phys.* **99**, 053511 (2006).
- <sup>7</sup>R. J. Bell and P. Dean, *Philos. Mag.* **25**, 1381 (1972).
- <sup>8</sup>P. H. Gaskell and I. D. Tarrant, *Philos. Mag. B* **42**, 265 (1980).
- <sup>9</sup>L. Guttman and S. M. Rahman, *Phys. Rev. B* **37**, 2657 (1988).
- <sup>10</sup>R. T. Haftka and Z. Gürdal, *Elements of Structural Optimization (Solid Mechanics and Its Applications)* (Kluwer, Dordrecht, 1992).
- <sup>11</sup>C. Yuan, G. Q. Zhang, L. J. Ernst, F. van Keulen, W. D. van Driel, R. B. R. van Silfhout, O. van der Sluis, and B. J. Thijsse, *Proceedings of the EuroSimE 2007*, London (IEEE, New York, 2007), pp. 35–40.
- <sup>12</sup>A. E. H. Love, *A Treatise on the Mathematical Theory of Elasticity* (Cambridge University Press, Cambridge, 1934).
- <sup>13</sup>Materials Studio-Discover, Accelrys, Inc., 2005.
- <sup>14</sup>H. Sun, *J. Phys. Chem. B* **102**, 7338 (1998).
- <sup>15</sup>K. Maex, M. R. Baklanov, D. Shamiryani, F. Iacopi, S. H. Brongersma, and Z. S. Yanovitskaya, *J. Appl. Phys.* **93**, 8793 (2003).
- <sup>16</sup>L. P. Koliyar and G. S. Springer, *Mechanics of Composite Structures* (Cambridge University Press, Cambridge, 2003).
- <sup>17</sup>G. Carlotti, P. Colpani, D. Piccolo, S. Santucci, V. Senez, G. Socino, and L. Verdini, *Thin Solid Films* **414**, 99 (2002).
- <sup>18</sup>J. Yim, Y. Lyu, H. Jeong, S. K. Mah, H. Jingyu, J. Hahn, G. Kim, S. Chang, and J. Park, *J. Appl. Polym. Sci.* **90**, 626 (2003).